Journal of
PERIODONTAL RESEARCH

J Periodont Res 2011; 46: 513–521

JOURNAL OF PERIODONTAL RESEARCH
doi:10.1111/j.1600-0765.2011.01351.x

Fiber system degradation, and periostin and connective tissue growth factor level reduction, in the periodontal ligament of teeth in the absence of masticatory load

J. W. Choi[1], C. Arai[2], M. Ishikawa[2], S. Shimoda[1], Y. Nakamura[2]

[1]Department of Oral Anatomy I, School of Dental Medicine, Tsurumi University, Tsurumi-ku, Yokohama, Japan and [2]Department of Orthodontics School of Dental Medicine, Tsurumi University, Tsurumi-ku, Yokohama, Japan

Choi JW, Arai C, Ishikawa M, Shimoda S, Nakamura Y. Fiber system degradation, and periostin and connective tissue growth factor level reduction, in the periodontal ligament of teeth in the absence of masticatory load. J Periodont Res 2011; 46: 513–521. © 2011 John Wiley & Sons A/S

Background and Objective: The periodontal ligament (PDL), which is interposed between the alveolar bone and roots, supports teeth against mechanical stress. Periostin and connective tissue growth factor (CTGF) might play essential roles in maintaining PDL fiber integrity under mechanical stress. However, this relationship has not been studied at the protein and gene levels. Therefore, the aim of this study was to assess the PDL fiber system without masticatory load to determine the structural changes in the PDL in the absence of mechanical stress.

Material and Methods: The study included 45 Wistar male rats (12 wk of age) whose upper-right first molars were relieved from occlusion for 24 h, 72 h, 7 d or 21 d. The PDL was examined histologically, and changes in the gene and protein levels of periostin and CTGF were investigated.

Results: The PDL space width was reduced significantly. Histologically, an initial reduction in the fiber number and thinning of PDL fibers were observed, followed by disarrangement of the PDL fibers and their attachments to the alveolar bone; finally, the PDL fibers lost their meshwork structure. Real-time RT–PCR results revealed sharp down-regulation of the periostin and CTGF mRNA levels at 24 and 72 h, respectively, which continued throughout the experiment. Immunohistochemical analysis revealed that periostin localized to both the cellular elements and the extracellular matrix, whereas CTGF localized only to the cellular elements. Periostin and CTGF immunoreactivities became very weak without masticatory load.

Conclusion: In the absence of mechanical stress, the PDL fiber system undergoes degradation concomitantly with a reduction in the periostin and CTGF levels in the PDL.

Jae-won Choi, School of Dental Medicine, Tsurumi University, 2-1-3, Tsurumi, Tsurumi-ku, Yokohama 230-8501, Japan
Tel: 045 581 1001
Fax: 045 582 8860
e-mail: choijaewon@tsurumi-u.ac.jp

Key words: periodontal ligament; periodontal fiber; periostin; connective tissue growth factor

Accepted for publication December 4, 2010

A ligament is a dense fibrous connective tissue that interconnects bones and maintains the structures of tissues and organs. Most ligaments are composed of parallel collagen fiber bundles that react in a flexible manner to changes in external pressure and adapt to the new environment by reconstructing their arrangement (1). The mechanical strength of ligaments is mainly derived from the regular arrangement of collagen fiber bundles (2). Many studies have shown that the biological reaction of a ligament to mechanical stress is similar to that of bone to mechanical stress; this phenomenon can be explained by the mechanostat theory (3).

The periodontal ligament (PDL) is a unique ligament that connects the alveolar bone to the cementum. It is rich in vascular and cellular elements, which distinguishes it from other ligaments (4,5). The PDL comprises five different fiber groups – the alveolar crest, horizontal, oblique, apical and inter-radicular fiber groups – that support the teeth under constant mechanical stress during mastication. Each fiber group forms a meshwork structure that maintains the integrity of the PDL. The fibers are anchored in the alveolar bone or in the cementum and are usually referred to as Sharpey's fibers (6). The functions of the PDL depend on its viscoelastic properties, which are attributable to the dense fiber meshwork structure that prevents tissue damage from an abrupt powerful external force.

The PDL is primarily composed of types I, III (7,8) and XII (9) collagen. Type I collagen is the main structural protein of collagen fibers, which are responsible for the mechanical properties of the PDL. Collagen fibrillogenesis is a complicated process in which many extracellular matrix (ECM) proteins are involved: tenascin-X (10), secreted protein acidic and rich in cysteine (SPARC) (11), periostin (12), connective tissue growth factor (CTGF) (13), fibronectin (14) and thrombospondin (11,15,16). Periostin can regulate the fibrillogenesis of type I collagen; therefore, periostin is an important mediator of the biomechanical properties of fibrous connective tissue (12) and is essential for maintaining the integrity of the PDL in response to mechanical stress (17). CTGF stimulates the synthesis of many ECM proteins, such as types I, III and XII collagen, tenascin-C and SPARC (18), in response to changes in mechanical stress. CTGF also up-regulates the expression of types I and III collagen, periostin and biglycan (13). Therefore, periostin and CTGF may play essential roles in maintaining the integrity of the PDL fiber system under mechanical stress.

Many studies have been conducted to assess the changes in the PDL under mechanical stress (9,19–22). However, no study has investigated the relationship between the PDL fiber system and mechanical stress at the protein and gene levels. In this study, we investigated the structural changes in the PDL fiber system of rat molars, and the changes in the periostin and CTGF levels in the PDL in the absence of mechanical stress.

Material and methods

Ethical approval

All animal studies were conducted with the approval of the Institutional Animal Care and Use Committee of the Tsurumi University School of Dental Medicine.

Animals

The study population included 45 male Wistar rats (Japan SLC, Hamamatsu, Japan), 12 wk of age. The rats were divided into two groups: the experimental group (without masticatory load, $n = 36$) and the control group [no treatment (normal occlusal load), $n = 9$]. The rats were housed in groups in standard vivarium cages and maintained on a 12 h light : 12 h dark cycle; they had *ad libitum* access to standard rat chow and water. The rats did not have gingival inflammation around the upper molars.

Experimental design

To induce changes in mechanical stress, the masticatory load on the upper right molars was eliminated by removing the crowns of the antagonistic teeth. Under ether anesthesia, the crowns of the lower right molars were cut using small pliers and ground using a dental bur. The rats in the experimental group were segregated into subgroups that were killed using pentobarbital sodium (Nembutal, 0.05 mL/100 g body weight; Daiichi Sankyo Co., Tokyo, Japan) anesthesia, 24 h, 72 h, 7 d or 21 d after crown removal.

Preparation for histological analysis

Phosphate-buffered formalin solution (10%, pH 7.2, 4°C) was perfused for 15 min through the ascending aortae of four rats each from the experimental and control groups. Their maxillae were dissected and immersed in the same fixative at 4°C overnight. After fixation, the maxillae were trimmed into small blocks containing the first molar, decalcified for 3 wk by immersion in EDTA-Na (5.0%, pH 7.2, 4°C) solution containing 7.0% sucrose, dehydrated using a graded ethanol series and embedded in paraffin. The tissue blocks were sectioned frontally (Fig. 1) to obtain serial, 5-μm-thick sections, which were then stained with hematoxylin and eosin or with azan to visualize the PDL fibers.

Preparation for immunohistochemistry and real-time PCR

Under pentobarbital sodium anesthesia, the maxillae of rats ($n = 5$) were excised and rapidly immersed in isopentane cooled with liquid nitrogen. The enamel above the gingival level was removed, and the frozen tissues were trimmed, using a dental diamond disc, into smaller blocks containing the first molar. The frozen tissues were then embedded in precooled OCT compound (Sakura Finetek Inc., Torrance, CA, USA) and returned to liquid nitrogen until the OCT compound was completely frozen. The frozen blocks from the five rats were then mounted on stubs precooled to −25°C in a cryostat (Leica Microsystems, Wetzlar, Germany) with OCT compound and sectioned frontally by

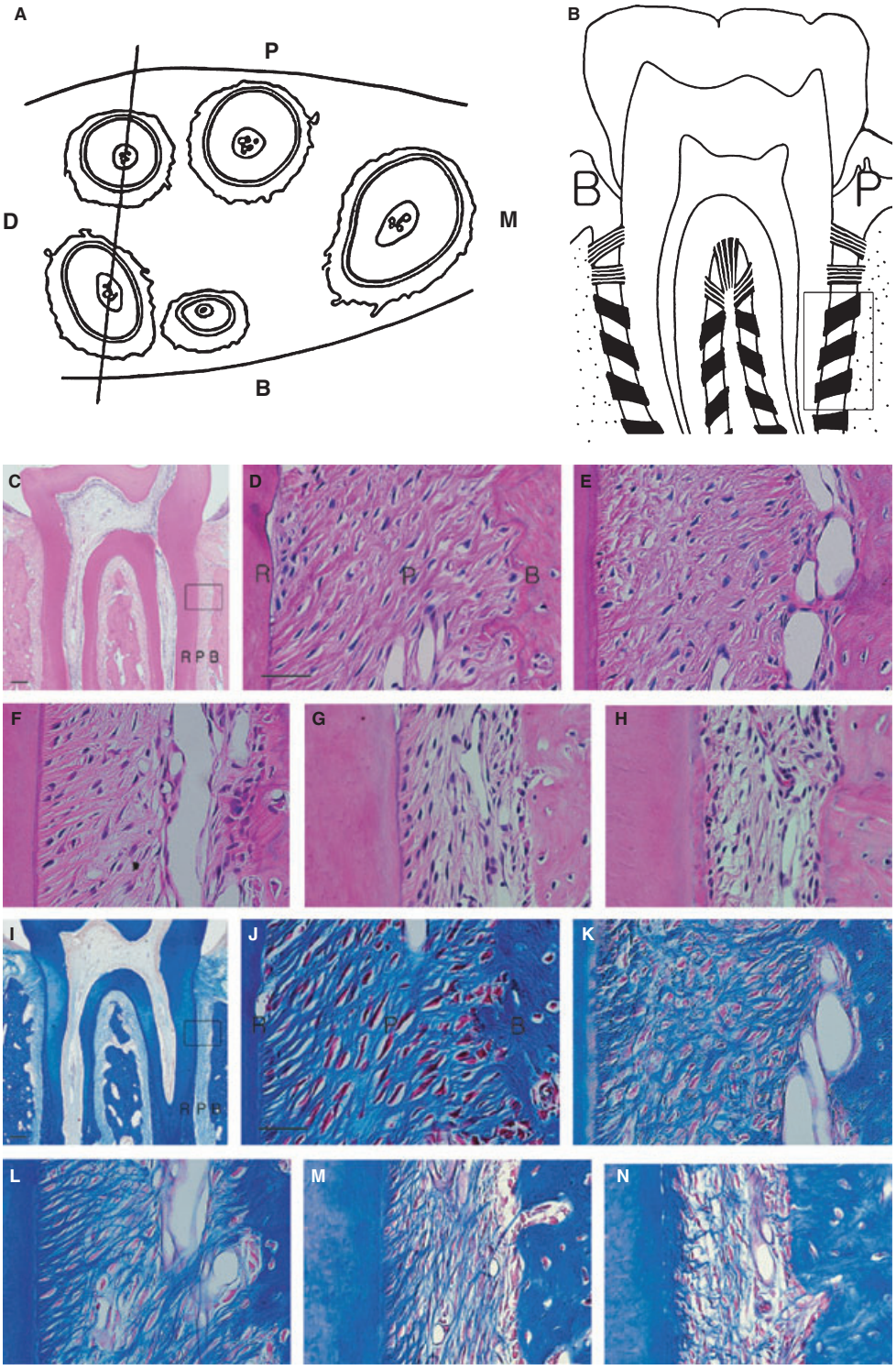

Fig. 1. Observation areas. (A) The frontal sections were cut parallel to the plane containing the distobuccal and distopalatal roots of the upper first molar. B, buccal; D, distal; M, mesial; P, palatal. (B) The oblique fibers were observed approximately 200 μm from the alveolar crest (boxed area) in the frontal sections. Hematoxylin and eosin-stained images of the periodontal ligament (PDL) during the experimental periods. (C) Frontal cross-section of the upper first molar. (D–H) Oblique fibers in the boxed area of (C). (D) Control group, (E) 24-h experimental group, (F) 72-h experimental group, (G) 7-d experimental group and (H) 21-d experimental group. B, alveolar bone; P, periodontal ligament; R, root of tooth. Scale bar, 20 μm; original magnification, 20 × (C) and 400 × (D–H). Azan-stained images of the PDL during the experimental periods. (I) Frontal cross-section of the upper first molar. (J–N) Oblique fibers in the boxed area of (I). (J) Control group, (K) 24-h experimental group, (L) 72-h experimental group, (M) 7-d experimental group and (N) 21-d experimental group. B, alveolar bone; P, periodontal ligament; R, root of tooth. Scale bar, 20 μm; original magnification, 20 × (I) and 400 × (J–N).

using a super-hard tungsten steel knife (Meiwa Shoji Ltd., Tokyo, Japan) (23). Serial, 7-μm-thick frontal sections were individually collected using powerful adhesive tape (using the Kawamoto method), then left for 1 h in the cryostat.

Immunohistochemistry

The frozen sections were fixed with 100% ethanol for 1 min, incubated in 3% H_2O_2 for 10 min to quench the endogenous peroxidase activity and then blocked with goat serum for 60 min at room temperature. Periostin and CTGF were detected using polyclonal rabbit primary antibodies (1:1000 dilution; Acris Antibodies GmbH, Herford, Germany, and Lifespan Biosciences, Inc., Seattle, WA, USA, respectively). The sections were incubated with the primary antibodies for 30 min, then with avidin-biotinylated horseradish peroxidase-conjugated secondary antibodies; the rabbit ABC staining system (Vector Laboratories, Burlingame, CA, USA) was used for this staining procedure.

Real-time PCR

RNA extraction Samples for total RNA extraction were obtained from the sections by using laser capture microdissection (LCM). In brief, the frozen sections were fixed with methanol for 3 min, stained with toluidine blue for 10 s and washed with distilled water. The PDL areas containing oblique fibers were microdissected from the sections by using the PALM MicroBeam system (PALM Microlaser Technologies AG, Bernried, Germany) equipped with a nitrogen laser (337 nm) for cutting, ablating and collecting the tissues using laser pressure catapulting technology. The margins for the irradiation zone were drawn a few cell layers away from the calcified bone and cementum in order to exclude osteoblasts and cementoblasts (Fig. 2). After LCM, the dissected samples were ejected from the object plane without mechanical contact and catapulted directly into a microfuge cap, using a single laser shot for subsequent RNA extraction. Total RNA was extracted using an RNeasy micro kit (Qiagen GmbH, Hilden, Germany).

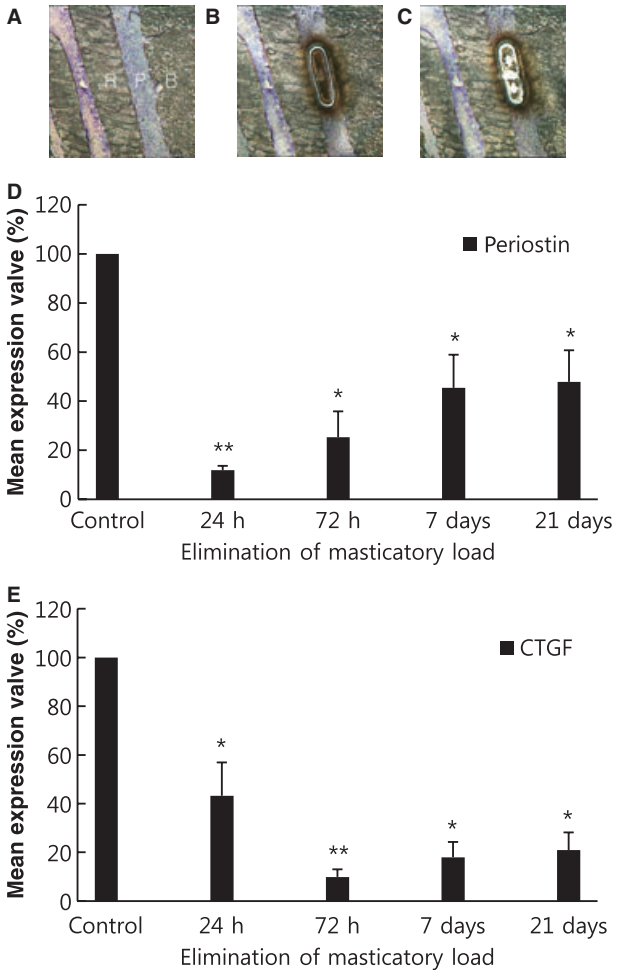

Fig. 2. Laser capture microdissection (LCM) of the periodontal ligament (PDL) in the frozen sections. (A) Before LCM. (B) The irradiation zone in the PDL is outlined on the section. (C) The outlined PDL area was obtained after laser pressure catapulting. B, alveolar bone; P, periodontal ligament; R, root of tooth. Scale bar, 100 μm; original magnification, 100 ×. Changes in the expression of mRNA for periostin (D) and connective tissue growth factor (*Ctgf*) (E) in the PDL during the experimental periods. The level of expression in the control group was set to 100% (relative expression). The data represent the mean ± standard deviation values of five rats per group after normalization to glyceraldehyde-3-phosphate dehydrogenase (*Gapdh*) mRNA expression. $*p < 0.05$ and $**p < 0.005$ vs. the control group, determined using the *t*-test.

One-step real-time RT-PCR A one-step real-time RT-PCR assay was performed for each target gene by using the total RNA samples and serial dilutions of known amounts of total RNA standards prepared for generating the standard curve. A One Step SYBR PrimeScript RT-PCR Kit II (Takara Bio Inc., Otsu, Japan) was used for this assay; the assay was performed using 96-well plates, in a Thermal Cycler Dice Real Time System (Takara Bio Inc.). The PCR conditions are given in Table 1.

For each sample, an amplification plot was generated, which showed an increase in the reporter dye fluorescence with each PCR cycle. A threshold cycle (C_t) value was calculated for each amplification plot; the C_t value is the PCR cycle at which fluorescence is detected above the threshold and is

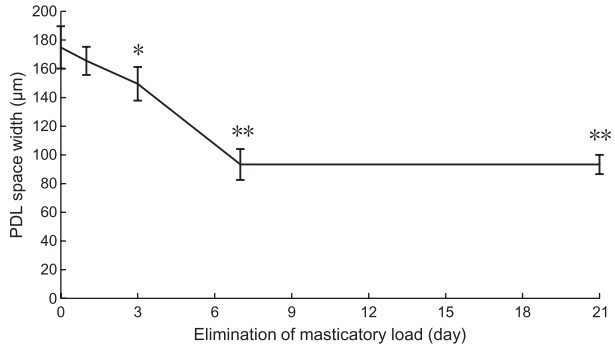

Fig. 3. Changes in the width of the periodontal ligament (PDL) space during the experimental periods. The data represent the mean ± standard deviation. *$p < 0.05$ and **$p < 0.005$ vs. the control group, determined using the *t*-test.

calculated on the basis of the variability of baseline data in the first 15 cycles. The C_t values were used to calculate the initial amount of target mRNA in the respective samples by using the line equations derived from the respective standard curves. A standard curve of the C_t values vs. the logarithmic values of the concentrations of the different dilutions of the total RNA standards was plotted for each gene. If a fluorescence signal was not detected within 45 cycles, the results were considered negative.

To correct for possible variability in the efficiency of the RT reactions, we performed PCR amplification for the housekeeping gene glyceraldehyde-3-phosphate dehydrogenase (GAPDH) and plotted the GAPDH standard curve. The endogenous *Gapdh* mRNA levels were quantified using the same procedure used for the target genes and were found to be identical among all the samples studied. Therefore, similarly to a previous study (24), we considered *Gapdh* mRNA to be an appropriate internal control and normalized the amount of target mRNA relative to the amount of *Gapdh* mRNA. In this study, the amount of target mRNA was represented by the normalized value (i.e. target mRNA/*Gapdh* mRNA).

Observation areas and measurement of PDL space width

The PDL areas containing oblique fibers were mainly used for the histological, immunohistochemical and real-time PCR analyses. The width of the PDL space was measured on the histological sections containing the distobuccal and distopalatal roots of the upper first molar by using an Olympus BX60 microscope (Olympus Co. Ltd., Tokyo, Japan) interfaced with an Olympus DP72 digital camera (Olympus Co. Ltd.).

Statistical analyses

The Student's *t*-test was used for comparisons between the control and each experimental group (SPSS® 11.0J; Chicago, IL, USA). The results for each group are represented in terms of mean ± standard deviation values; and $p < 0.05$ and $p < 0.005$ were considered statistically significant.

Results

Changes in body weight

The initial body weight of the animals was almost the same between the experimental and control groups, ranging from 315 to 352 g. Although a slight reduction in weight was observed in the experimental group 24 h after crown removal, the overall average weights of the rats in the experimental and control groups increased, and the overall proportional increments in body weight were quite similar between the experimental groups and control groups. Consequently, no significant difference was found between the weights of the rats of the two groups.

Histological findings

Three types of PDL fibers were observed in the control group (Fig. 1C and 1I): alveolar crest fibers, horizontal fibers and oblique fibers. The fibers that connected the tooth to the alveolar bone were stretched and interlaced in a dense meshwork structure; they exhibited the normal regular arrangement of PDL fibers under masticatory load (25). Fibroblasts were observed throughout the PDL and were scattered along the fibers (Fig 1C and 1D). Osteoblasts and cementoblasts were observed among the PDL fibers on the surfaces of the bone and cementum, respectively (Fig 1C and 1D).

Table 1. Primers and cycling conditions in real-time RT-PCR analysis

Gene	Primer sequence (5′ → 3′)		Annealing temperature (°C)	No. of cycles	Product length (bp)
Periostin	Forward	AGGAGCGGTGTTTGAGACCAT	58	45	203
	Reverse	GTGAAAGTGGTTTGCTGTTT			
Ctgf	Forward	ATGATGCGAGCCAAGTGCCTG	60	45	198
	Reverse	CGGATGCACTTTTTGCCCTTCTTAATG			
Gapdh	Forward	CAACTCCCTCAAGATTGTCAGCAA	60	45	113
	Reverse	GGCATGGACTGTGGTCATGA			

Ctgf, connective tissue growth factor; *Gapdh*, glyceraldehyde-3-phosphate dehydrogenase.

In the experimental group, the characteristics of the PDLs of the rats in the 24-h group were very similar to those of the control group (i.e. the PDLs in both groups had almost the same width, number of PDL fibers and cell arrangement (Fig. 1D, 1E, 1J and 1K). However, the PDL space in the rats of the 72-h experimental group was significantly narrower than that in the rats of the control group; in addition, the PDL fibers of the rats in the 72-h experimental group seemed to be thinner than those of the rats in the control group ($p < 0.05$) (Figs 1F, 1L and 3). The fiber meshwork structure was somewhat looser in the PDLs of the rats from the 72-h experimental group. In the 7-d experimental group, the width of the PDL space narrowed to less than two-thirds of the width of the PDL space in the control group, and the PDL fibers became noticeably thinner than those of the rats in the 72-h experimental group ($p < 0.005$) (Figs 1G, 1M and 3). The meshwork structure was apparently lost, with a marked reduction observed in the number of fibers and in the fiber attachments to the alveolar bone (Fig. 1M). The arrangement of the fibroblasts was different from that in the control group (i.e. the fibroblasts in the experimental group were arranged parallel to the tooth surface) (Fig. 1G and 1M). Osteoblasts occupied most of the bone surface, and a further reduction in the number of PDL fibers and fiber attachments was observed (Fig. 1G and 1M). After 21 d, the width of the PDL space in the rats from the experimental group narrowed to less than half of that in the rats from the control group ($p < 0.005$) (Figs 1H, 1N and 3). The bone surface was unchanged, but fewer PDL fibers were attached to the cementum. The dense meshwork structure disappeared with loss of fiber attachment to the bone and cementum (Fig. 1H and 1N).

Real-time PCR analysis

The periostin mRNA level was sharply down-regulated in the experimental 24-h group ($p < 0.005$) and then gradually increased during the course of the experiment ($p < 0.05$) (Fig. 2D and 2E); however, the periostin mRNA expression levels in this experimental group remained significantly lower than those of the corresponding control group ($p < 0.05$). The level of *Ctgf* mRNA was also sharply down-regulated in the experimental 24-h group ($p < 0.05$) and decreased further until 72 h ($p < 0.005$) (Fig. 2D and 2E). A slight increase was then observed over the course of the experiment, but the expression levels of *Ctgf* mRNA in this experimental group were significantly lower than those of the control group ($p < 0.05$).

Immunohistochemical analysis

Periostin immunoreactivity was observed throughout the PDL (Fig. 4). Periostin was localized not only to the cellular elements but also to the ECM. The immunoreactivity in the experimental 24-h group was similar to that in the control group. The periostin immunoreactivity in the rats from the 72-h experimental group was very weak compared with that of the rats from the control group, and the immunoreactivities in the rats from the 7- and 21-d experimental groups were also weak compared with those in the

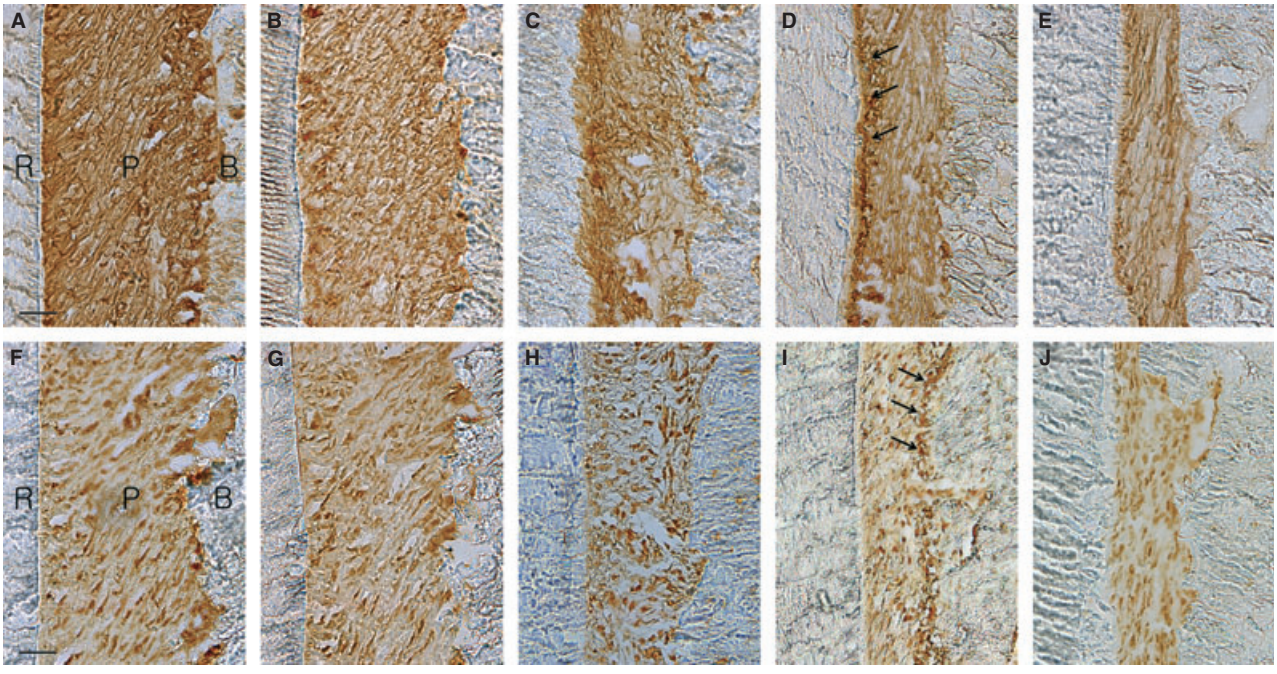

Fig. 4. Immunostaining of periostin (A–E) and connective tissue growth factor (CTGF) (F–J) in the periodontal ligament (PDL) during the experimental periods. (A, F) 0 h, (B, G) 24-h experimental group, (C, H) 72-h experimental group, (D, I) 7-d experimental group and (E, J) 21-d experimental group. The arrows indicate areas of strong expression of periostin and CTGF. B, alveolar bone; P, periodontal ligament; R, root of tooth. Scale bar, 40 μm; original magnification, 400 ×.

rats from the control groups; the bone surface exhibited weak immunoreactivity, which was lower than that exhibited by the cemental surface.

The distribution pattern for CTGF immunoreactivity was a little different from that for periostin immunoreactivity. CTGF was localized only to the cellular elements in the PDL (Fig. 4). In the control group, intense immunoreactivity was observed in the osteoblasts at the bone surface, but no immunoreactivity was observed in the cementoblasts. The PDLs of the rats in the experimental group showed weak immunoreactivity 24 h after the removal of the antagonistic tooth. The immunoreactivity was even weaker in the 72-h experimental group and remained weak in the 7- and 21-d experimental groups. Although the immunoreactivity of the osteoblasts on the bone surface was weak, it was higher than that of the other cellular elements.

Discussion

Masticatory loading can be eliminated by various methods, such as resection of the masticatory muscles (26), use of a soft diet (27), removal of occlusal contacts (20,28,29) and extraction of antagonistic teeth (21,22,30). In this study, the crowns of the lower right molars were removed to eliminate masticatory load on the upper right molars. Although this procedure caused slight tooth elongation, the upper first molar did not contact the lower gingiva during the experimental period (22,30). Therefore, this method seems to be reliable for inducing stress-free conditions for teeth.

In the current study, we mainly studied the oblique fiber areas. This is because the oblique fiber areas have the greatest number of fibers and support the tooth against the vertical pressure force during mastication. The changes in the fiber system in the oblique fiber areas were also observed in the other areas of the PDL. Fiber system degradation is a commonly observed change in the PDL. Therefore, it is reasonable that the immunohistochemical findings for the oblique fiber area were similar to those for the other areas of the PDL.

Previously, we reported that LCM is useful for obtaining data on specific areas of the PDL and for analyzing mRNA expression levels in the PDL *in vivo* (31,32). In the previous studies, as well as in the current study, we used LCM to obtain samples from the oblique fiber group in the PDL for one-step real-time RT-PCR analysis. This allowed us to accurately quantify the comprehensive data obtained for gene-expression levels in PDL *in vivo*. Glickman reported the presence of elongated bone trabeculae along the margin of the alveolar bone after removal of the antagonist (28). In their calcein-labeling study, Levy and Mailland reported that the narrowing of the PDL space is caused by bone formation on the alveolar wall (33). In the current study, we found significant reduction (to less than half of the normal width) in the width of the PDL space. The reduction in the PDL space was probably caused by bone formation on the alveolar bone surface because the thickness of the cementum in the oblique fiber areas changed little, and may also be related to the narrow range of tooth mobility, which was caused by the elimination of masticatory load. A tooth does not require a wide PDL space when it is not subjected to constant mechanical stress.

In the absence of masticatory load, bone formation was observed on the alveolar bone surface, whereas under the same conditions, the PDL fibers underwent degradation. The fiber meshwork structure was lost over the course of the experiment in the following sequence: the PDL fibers were first disarranged and then thinned, and then the number of fibers was reduced and a reduction in attachment of the fiber to the bone was observed. Most of the fibers separated from the bone. These results indicate that the tooth-supporting capacity of the PDL decreased remarkably. These findings were commonly observed in the other areas of the PDL, such as the horizontal fiber groups and the apical fiber groups. The changes observed are characteristic of disuse atrophy and are very similar to the findings for bone tissue in the absence of mechanical stress. The PDL reaction in this study appears to reflect the mechanostat theory of bone tissue (3), although the PDL reaction was much more rapid than that of the bone tissue (34).

The results clearly indicated significant down-regulation of periostin and CTGF in the unloaded PDL. The immunohistochemical results also showed reduced periostin immunoreactivity in the absence of masticatory load. Periostin is predominantly expressed in collagen-rich fibrous connective tissue that is subjected to constant mechanical stress, and periostin expression is always up-regulated in response to overloading (12,19,35,36). The results of many studies revealed that periostin is an essential factor in the PDL (17,35). Furthermore, Norris *et al.* reported that periostin binds directly to collagen type I (12). These findings indicate that periostin is closely related to the regulation of the PDL through type I collagen fibrillogenesis and the assembly of collagen fibrils. Histological findings (i.e. loss of the meshwork structure, a decrease in the number of PDL fibers and a decrease in the thickness of the PDL fibers) indicate deterioration of the fiber system, which is closely related to the down-regulation of periostin. This suggests that the periostin protein is also involved in the formation of the meshwork structure of the PDL fibers. Interestingly, immunohistochemical analysis of periostin revealed differences in the immunoreactivity of the bone and cementum surfaces, for instance, the bone surface showed lower immunoreactivity than did the cementum surface. This may be caused by the decrease in the number of PDL fibers (Sharpey's fibers) on the bone surface, indicating that periostin may play an important role in maintaining the PDL fibers on the bone surface. A slight increase in the periostin expression level after sharp down-regulation at 24 h suggests PDL adaptation to the absence of masticatory load (i.e. the unloaded condition), in which less periostin is required to maintain the PDL than that required in the presence of a masticatory load.

The real-time PCR results also showed a significant reduction in CTGF expression in the PDL. This

reduction was confirmed by the immunohistochemical results. The gene encoding CTGF shows the greatest up-regulation among all the genes expressed in tissue in the presence of mechanical stress; this mechanical stress is essential for a high level of expression of CTGF (18,37,38). In a recent study, mechanical stimuli led to the induction of connective tissue synthesis and to the simultaneous inhibition of matrix degradation in human fibroblasts (39). It is reasonable to consider that the down-regulation of CTGF in this study was caused by the lack of mechanical stress and consequently influenced the synthesis of type I collagen in the fibroblasts. This down-regulation influences the collagen turnover and leads to significant degradation of collagen in the PDL fibers, explaining the reduced number of PDL fibers and loss of their meshwork structure. Unlike the findings for periostin, the immunohistochemical results revealed differences in the immunoreactivity between the bone and the cemental surfaces. The bone surface showed higher immunoreactivity than did the cemental surface. The higher immunoreactivity is related to bone formation on the alveolar surface. These results indicate that CTGF plays an important role in maintaining the homeostasis of the PDL under mechanical stress and bone formation.

In this study, the mRNA expression levels of periostin and CTGF are different in time-dependent changing pattern. This suggests that periostin and CTGF were differently regulated in the fibroblasts in the PDL in response to elimination of masticatory load. In conclusion, the results showed that the PDL fiber system undergoes degradation concomitantly with reduction in the periostin and CTGF levels in the PDL of teeth in the absence of mechanical stress (masticatory load); however, the precise roles of periostin and CTGF need to be further investigated. In particular, further research is required to elucidate the function of changes in the temporal expression of periostin and CTGF under mechanical stress, such as that created by orthodontic force.

Acknowledgements

We would like to acknowledge Professor K. Kawasaki (honorary professor, Department of Oral Anatomy I) for his support and encouragement throughout the present study. This study was supported in part by a Grant-in-Aid for Scientific Research (C) (17592153) from the Ministry of Education, Science, Sports and Culture of Japan.

References

1. Berkovitz BK. The structure of the periodontal ligament: an update. *Eur J Orthod* 1990;**12:**51–76.
2. Bosshardt DD, Selvig KA. Dental cementum: the dynamic tissue covering of the root. *Periodontol 2000* 1997;**13:**41–75.
3. Frost HM. The Utah paradigm of skeletal physiology: an overview of its insights for bone, cartilage and collagenous tissue organs. *J Bone Miner Metab* 2000;**18:**305–316.
4. Everts V, van derZee E, Creemers L, Beertsen W. Phagocytosis and intracellular digestion of collagen, its role in turnover and remodelling. *Histochem J* 1996; **28:**229–245.
5. Sims MR, Leppard PI, Sampson WJ, Dreyer CW. Microvascular luminal volume changes in aged mouse periodontal ligament. *J Dent Res* 1996;**75:**1503–1511.
6. Kurihara S, Enlow DH. An electron microscopic study of attachments between periodontal fibers and bone during alveolar remodeling. *Am J Orthod* 1980;**77:** 516–531.
7. Butler WT, Birkedal-Hansen H, Beegle WF, Taylor RE, Chung E. Proteins of the periodontium. Identification of collagens with the [alpha1(I)]2alpha2 and [alpha1(III)]3 structures in bovine periodontal ligament. *J Biol Chem* 1975;**250:** 8907–8912.
8. Huang YH, Ohsaki Y, Kurisu K. Distribution of type I and type III collagen in the developing periodontal ligament of mice. *Matrix* 1991;**11:**25–35.
9. Karimbux NY, Nishimura I. Temporal and spatial expressions of type XII collagen in the remodeling periodontal ligament during experimental tooth movement. *J Dent Res* 1995;**74:**313–318.
10. Minamitani T, Ariga H, Matsumoto K. Deficiency of tenascin-X causes a decrease in the level of expression of type VI collagen. *Exp Cell Res* 2004;**297:**49–60.
11. Bradshaw AD, Puolakkainen P, Dasgupta J, Davidson JM, Wight TN, Helene Sage E. SPARC-null mice display abnormalities in the dermis characterized by decreased collagen fibril diameter and reduced tensile strength. *J Invest Dermatol* 2003;**120:**949–955.
12. Norris RA, Damon B, Mironov V *et al.* Periostin regulates collagen fibrillogenesis and the biomechanical properties of connective tissues. *J Cell Biochem* 2007; **101:**695–711.
13. Dangaria SJ, Ito Y, Walker C, Druzinsky R, Luan X, Diekwisch TG. Extracellular matrix-mediated differentiation of periodontal progenitor cells. *Differentiation* 2009;**78:**79–90.
14. Li S, Van Den Diepstraten C, D'Souza SJ, Chan BM, Pickering JG. Vascular smooth muscle cells orchestrate the assembly of type I collagen via alpha2beta1 integrin, RhoA, and fibronectin polymerization. *Am J Pathol* 2003;**163:**1045–1056.
15. Kyriakides TR, Zhu YH, Smith LT *et al.* Mice that lack thrombospondin 2 display connective tissue abnormalities that are associated with disordered collagen fibrillogenesis, an increased vascular density, and a bleeding diathesis. *J Cell Biol* 1998;**140:**419–430.
16. Bornstein P, Armstrong LC, Hankenson KD, Kyriakides TR, Yang Z. Thrombospondin 2, a matricellular protein with diverse functions. *Matrix Biol* 2000;**19:** 557–568.
17. Rios HF, Ma D, Xie Y *et al.* Periostin is essential for the integrity and function of the periodontal ligament during occlusal loading in mice. *J Periodontol* 2008;**79:** 1480–1490.
18. Schild C, Trueb B. Mechanical stress is required for high-level expression of connective tissue growth factor. *Exp Cell Res* 2002;**274:**83–91.
19. Afanador E, Yokozeki M, Oba Y *et al.* Messenger RNA expression of periostin and Twist transiently decrease by occlusal hypofunction in mouse periodontal ligament. *Arch Oral Biol* 2005;**50:**1023–1031.
20. Cohn SA. Disuse atrophy of the periodontium in mice following partial loss of function. *Arch Oral Biol* 1966;**11:**95–105.
21. Koike K. The effects of loss and restoration of occlusal function on the periodontal tissues of rat molar teeth: histopathological and histometrical investigation. *J Jpn Soc Periodont* 1996;**38:**1–19.
22. Suzuki S. The studies on changes of the periodontal tissues under the occlusal abnormality of experiment–traumatic occlusion and occlusion with the loss of antagonistic tooth. *Shigaku* 1978;**65:**817–857.
23. Nakamura Y, Tanaka T, Wakimoto Y, Noda K, Kuwahara Y. Preparation of unfixed and undecalcified frozen sections of adult rat periodontal ligament during experimental tooth movement. *Biotech Histochem* 1994;**69:**186–191.

24. Arai C, Ohnuki Y, Umeki D, Hirashita A, Saeki Y. Effects of clenbuterol and cyclosporin A on the myosin heavy chain mRNA level and the muscle mass in rat masseter. *J Physiol Sci* 2006;**56:**205–209.
25. Ten Cate AR, Deporter DA, Freeman E. The role of fibroblasts in the remodeling of periodontal ligament during physiologic tooth movement. *Am J Orthod* 1976;**69:**155–168.
26. Horowitz SL, Shapiro HH. Modifications of mandibular architecture following removal of temporalis muscle in the rat. *J Dent Res* 1951;**30:**276–280.
27. Watt DG, Williams CH. The effects of the physical consistency of food on the growth and development of the mandible and the maxilla of the rat. *Am J Orthod* 1951;**37:** 895–928.
28. Glickman I. The effect of acute starvation upon the apposition of alveolar bone associated with the extraction of functional antagonists. *J Dent Res* 1945;**24:** 155–160.
29. Masuda Y. Changes of the periodontal fibers following the experimental traumatic occlusion and the loss of antagonistic teeth. *Shigaku* 1971;**58:**794–829.
30. Saeki M. Experimental disuse atrophy and its repairing process in the periodontium of the rat molar. *J Stomatol Soc Jpn* 1959;**26:**317–347.
31. Nakamura Y, Nomura Y, Arai C *et al*. Laser capture microdissection of rat periodontal ligament for gene analysis. *Biotech Histochem* 2007;**82:**295–300.
32. Arai C, Nomura Y, Ishikawa M *et al*. HSPA1A is upregulated in periodontal ligament at early stage of tooth movement in rats. *Histochem Cell Biol* 2010;**134:**337–343.
33. Levy GG, Mailland ML. Histologic study of the effects of occlusal hypofunction following antagonist tooth extraction in the rat. *J Periodontol* 1980;**51:**393–399.
34. Sodek J. *A co*mparison of the rates of synthesis and turnover of collagen and non-collagen proteins in adult rat periodontal tissues and skin using a microassay. *Arch Oral Biol* 1977;**22:**655–665.
35. Rios H, Koushik SV, Wang H *et al*. *periostin* null mice exhibit dwarfism, incisor enamel defects, and an early-onset periodontal disease-like phenotype. *Mol Cell Biol* 2005;**25:**11131–11144.
36. Snider P, Hinton RB, Moreno-Rodriguez RA *et al*. Periostin is required for maturation and extracellular matrix stabilization of noncardiomyocyte lineages of the heart. *Circ Res* 2008;**102:**752–760.
37. Hishikawa K, Oemar BS, Nakaki T. Static pressure regulates connective tissue growth factor expression in human mesangial cells. *J Biol Chem* 2001;**276:** 16797–16803.
38. Yamashiro T, Fukunaga T, Kobashi N *et al*. Mechanical stimulation induces CTGF expression in rat osteocytes. *J Dent Res* 2001;**80:**461–465.
39. Kessler D, Dethlefsen S, Haase I *et al*. Fibroblasts in mechanically stressed collagen lattices assume a ''synthetic'' phenotype. *J Biol Chem* 2001;**276:**36575–36585.